Chemical Engineering Journal 198–199 (2012) 18–26

Contents lists available at SciVerse ScienceDirect

Chemical Engineering Journal

journal homepage: www.elsevier.com/locate/cej

Catalytic oxidation of carbon tetrachloride on metal exchanged Y-zeolite

S.A. Regenhardt [a], C.I. Meyer [a], A.F. Trasarti [a], A. Monzón [b], T.F. Garetto [a,*]

[a] GICIC-Instituto de Investigaciones en Catálisis y Petroquímica (INCAPE), FIQ-UNL-CONICET, Santiago del Estero 2654, 3000 Santa Fe, Argentina
[b] Department of Chemical and Environmental Engineering, Institute of Nanoscience of Aragon (INA), University of Zaragoza, 50009 Zaragoza, Spain

HIGHLIGHTS

- Y-Co catalyst is active and stable in carbon tetrachloride oxidation.
- The presence of water in the feed is necessary to avoid the catalyst deactivation.
- Kinetics results are consistent with a mechanism double site LHHW.
- O_2 and CCl_4 are adsorbed on different type of sites.

ARTICLE INFO

Article history:
Received 4 April 2012
Received in revised form 15 May 2012
Accepted 18 May 2012
Available online 27 May 2012

Keywords:
Carbon tetrachloride combustion
Exchanged Y-zeolite
Co-zeolite
Langmuir–Hinshelwood mechanism
Kinetic modeling

ABSTRACT

In this contribution we present the results of a kinetic study of the catalytic combustion of carbon tetrachloride over several catalysts of Y-zeolite exchanged with Cr, Co, Mn and Fe. The catalysts were prepared by ion exchange and characterized, before and after catalytic tests, by atomic absorption, N_2 physisorption (BET surface measurement) and X-ray diffraction.

The experimental results have been analyzed using both empirical, -power-law pseudo-homogenous-, and mechanistical -Langmuir–Hinshelwood-models. The catalytic results indicate the following order of activity: Y-Co > Y-Cr ≫ Y-Fe ≅ Y-Mn. According to the mechanism assumed to explain the kinetic results obtained, the oxygen molecule adsorbs over the surface Co^{++} species, and the carbon tetrachloride interacts with the H^+ ion on the Brönsted acid site. It was also obtained that the presence of water in the feed is necessary to avoid the deactivation of the catalyst. This effect is probably due to the capacity of water to restore the Brönsted acid sites depleted during the reaction.

1. Introduction

Chlorinated volatile organic compounds are used in the chemical industry for many purposes such as plastics manufacture, cleaning solvents and heat-transfer fluid [1]. Due to their suspected toxicity and carcinogenic properties effective methods to destroy the chlorinated volatile organic compounds are required. Thermal incineration of these compounds requires high temperatures, over 1000 °C, with the consequently high energy consumption. Among the alternative destruction techniques, the catalytic oxidation can transform the chlorinated compounds in CO_2, water and chlorine gas. As regards the chlorinated hydrocarbons such as methyl chloride (CH_3Cl), methylene chloride (CH_2Cl_2), chloroform ($CHCl_3$) and carbon tetrachloride (CCl_4), the compound that is the most difficult to destroy is the carbon tetrachloride [2]. Thus, some chlorinated compounds, such as, 1,2-dichloroethane, can be eliminated by combustion using acid catalysts [3]. However, it has been proposed [4–6] the necessity of using metallic catalysts based on exchanged zeolites, such as Co-Y or Cr-Y, to carry out the total oxidation of chlorinated volatile organic compounds.

One of the most important problems raised during these suited is the deactivation of the catalysts caused by the reactants, or by the products obtained, e.g. Cl_2 [5]. On the other side, in order to study the interaction between the chlorinated volatile organic compounds and the catalyst surface, the effect of the presence of water in the feed, or molecules that contain hydrogen have been studied [3]. Thus, López-Fonseca et al. [7] prepared a series of dealuminated zeolites which then were evaluated in the catalytic oxidation of dichloroethane and trichloroethylene. The activity increases when the dealumination increases until 50%. The authors related the increase in the activity with the strong acidity due to dealumination. Some papers propose different models in order to obtain the kinetic parameters [8,9]. In a previous paper we studied the kinetic behavior of exchanged zeolite in the combustion of trichloroethylene [10]. It was found that the kinetic data were consistent with an Eley–Rideal mechanism where the trichloroethylene molecule is reacting from the gas phase with the oxygen previously adsorbed. The aim of this work is to study the catalytic and kinetic behavior of a series of Y zeolite exchanged with Co, Cr, Mn and Fe

* Corresponding author. Tel.: +54 342 4533858; fax: +54 342 4531068.
E-mail address: tgaretto@fiq.unl.edu.ar (T.F. Garetto).

1385-8947/$ - see front matter © 2012 Elsevier B.V. All rights reserved.
http://dx.doi.org/10.1016/j.cej.2012.05.055

Nomenclature

r_{CCl_4}	reaction rate of CCl_4 oxidation (mol CCl_4 g_{cat}^{-1} h^{-1})
k_P	kinetic constant according to potential model
p_{O_2}	oxygen partial pressure (atm)
p_{CCl4}	CCl_4 partial pressure (atm)
α	reaction order respect to O2
β	reaction order respect to CCl_4
K_{O_2}	equilibrium constant of oxygen adsorption (SS-LHHW)
K_{H_2O}	equilibrium constant of water adsorption (SS-LHHW)
K_{CCl4}	equilibrium constant of CCl_4 adsorption (SS-LHHW)
p_{H_2O}	water partial pressure (atm)
$*_T$	total adsorption sites, considering only one type adsorption (SS-LHHW)
$*$	free adsorption sites (SS-LHHW)
S_T	adsorption sites corresponding to sites adsorption of water and oxygen (DS-LHHW)
S	free adsorption sites (DS-LHHW)
L_T	adsorption sites corresponding to CCl_4 adsorption (DS-LHHW)
L	free adsorption sites (DS-LHHW)
T	temperature (K)
T_m	reparameterization temperature (K)
k_{p_0}	pre-exponential factor defined in Eq. (4)
E_a	apparent activation energy (kJ mol^{-1})
SSR	sum of squared residuals
SE	standard error
R^2	correlation coefficient
$K_{O_2}^S$	equilibrium constant of oxygen adsorption (DS-LHHW)
$K_{H_2O}^S$	equilibrium constant of water adsorption (DS-LHHW)
K_{CCl4}^L	equilibrium constant of CCl_4 adsorption (DS-LHHW)
k_{SS}	intrinsic kinetic constant for SS-LHHW model (Eq. (8))
k'_{SS}	constant defined in Eq. (12)
k''_{SS}	constant defined in Eq. (15)
K'_{CCl4}	constant defined in Eq. (12)
k'_{O_2}	constant defined in Eq. (15)
n	number of experimental data (Eq. (3b))
p	number of parameters (Eq. (3b))
k_{DS}	intrinsic kinetic constant for DS-LHHW model (Eq. (20))
k'_{DS}	constant defined in Eq. (25)
k''_{DS}	constant defined in Eq. (28)

during the carbon tetrachloride combustion. This paper deals on the development of mathematical relationships between "potential" and "Langmuir Hinshelwood Hougen Watson" (LHHW) kinetic models, which facilitates the discrimination of the models used.

The kinetic study was carried out in order to evaluate the more plausible reaction mechanism that can explain satisfactorily the experimental results.

2. Experimental

2.1. Catalyst preparation and characterization

The four samples studied were prepared by ion exchange of a commercial Y-zeolite (Zeolyst) with a BET surface area of 720 m^2 g^{-1}. As was described previously, the exchange procedure was carried out employing proper solutions of nitrates of Co, Cr, Mn and Fe [10]. The samples obtained were named as Y-Co, Y-Cr, Y-Mn and Y-Fe respectively. The zeolite exchanged with Co was subjected to three successive steps of exchange, the Y-Cr sample was prepared using two steps, and the Y-Fe and Y-Mn samples only needed one exchange step. After that, the samples were dried overnight at 100 °C and then calcined at 500 °C in air for 2 h. Metal loadings were determined by atomic absorption spectrometry. The specific surface areas (*Sg*) were measured by N_2 physisorption at −196 °C, using a Autosorb 1-C sorptometer and BET analysis methods. Previous to N_2 physisorption, samples were degassed for 2 h at 200 °C under high vacuum conditions. The crystalline structure of solid samples were determined by powder X-ray diffraction (XRD) technique employing a Shimadzu diffractometer XD–D1 equipped with a monochromated Cu Kα radiation source.

2.2. Catalytic tests

The oxidation of CCl_4 was carried out in a fixed-bed tubular reactor (Pyrex, 0.8 cm i.d.) operating at atmospheric pressure. The liquid CCl_4 was fed by means of a syringe pump, which allows the use of variable flows of reactant. Before the reaction zone there is a preheater where the water and CCl_4 are vaporized. Catalytic tests were performed using catalyst loadings (*W*) of 0.5 g, contact times ($W/F^0_{CCl_4}$) of 96 g h mol^{-1} and gas flow rates of 500 mL min^{-1}. Catalytic tests were performed with or without water in the feed with a partial pressure of 0.03 atm that was kept constant for all experiments. Samples were sieved to retain particles within 0.35–0.42 mm diameter and then loaded to the reactor. The particle size used ensures the absence of any diffusional limitation, as was verified for several catalytic runs [10]. Before catalyst activity measurements, all the samples were activated in air at 500 °C for 1 h and then cooled to the desired reaction temperature. The gaseous stream was analyzed on-line using a Varian 3380 GC equipped with an FID detector and a packed Chromosorb 102 column 1/8″ × 3 m. Prior to the chromatographic analysis, the reactor outlet, containing the reaction products and non-converted reactants, was bubbled in a NaOH solution with methyl orange indicator in order to absorb the generated HCl. The reaction was followed through the conversion of CCl_4. Two types of experiments were performed: (i) measurement of CCl_4 conversion as a function of reaction temperature and (ii) measurement of the CCl_4 conversion as a function of time, under isothermal differential conditions.

3. Results and discussion

3.1. Catalyst characterization

The values of specific surface area (*Sg*), and cation loadings of the samples, before and after reaction, are given in Table 1. The number of exchanges for each catalyst were done in order to preserve the zeolite structure [10]. It can be observed that after the exchange, the *Sg* values are lower than those of the base zeolite. In

Table 1
Main characterization results of the catalysts.

Sample	% cation[a]	S_g (m^2/g)[a]	S_g (m^2/g)[b]	S_g (m^2/g)[c]	% cation[c]
Y	–	720	–	–	
Y-Co	4.20	590	40.0	558	4.15
Y-Cr	2.50	620	8.0	603	2.25
Y-Mn	4.15	618	7.50	591	4.06
Y-Fe	2.60	610	6.40	562	2.35

[a] Before catalytic reaction.
[b] After catalytic reaction without water added.
[c] After catalytic reaction with water added in the feed.

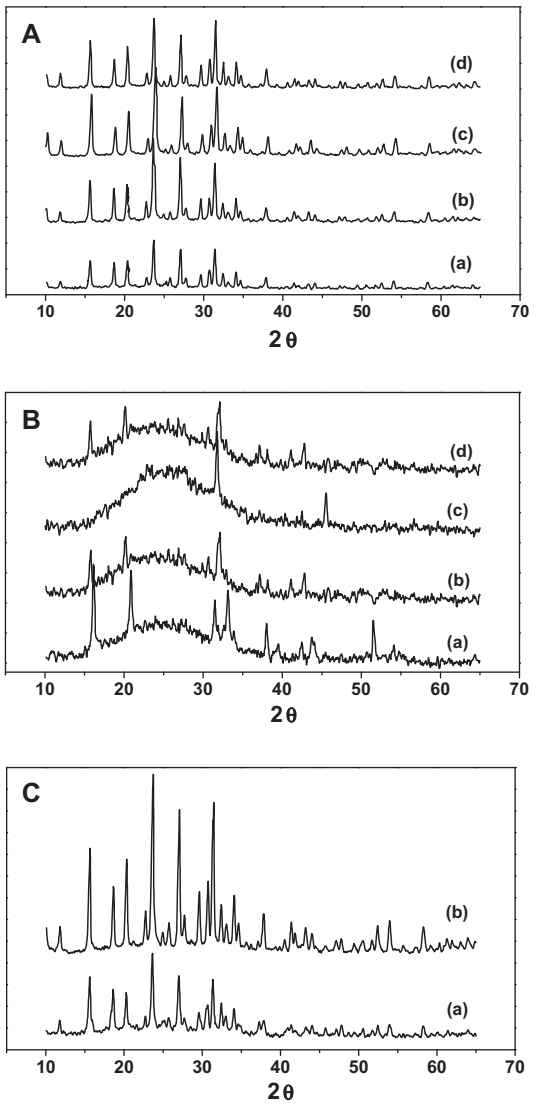

Fig. 1. X-ray diffraction patterns of exchanged zeolite corresponding to: fresh samples (A), after reaction, without water in the feed (B), after reaction with water in the feed (C). (a) Y-Co, (b) Y-Cr, (c) Y-Fe (d) Y-Mn.

Fig. 1A X-ray diffraction patterns are presented. It can be seen that the cristallinity of the samples was slightly affected by the exchange procedure. This diminution in the cristallinity of the samples is consistent with the decrease in the *Sg* values already mentioned. Similar behavior was observed in the same type of samples submitted to two or three exchanges [10]. It was not observed diffraction lines corresponding to the Co, Cr, Mn and Fe oxides due to the low loading of these cations.

3.2. Catalytic activity in absence of water in the feed

In Fig. 2 is presented the evolution of CCl_4 conversion with the reaction temperature for Y-Co and Y-Cr catalysts. In this case, the reaction was carried out without addition of water in the feed. Y-Mn and Y-Fe samples were not active at operating conditions employed. For both catalysts, Y-Co and Y-Cr, the CCl_4 conversion reaches a maximum decreasing strongly after that point. In the case of Y-Co the maximum conversion reached was 22% at 150 °C, and for the Y-Cr sample the maximum was 10% of conversion at 250 °C, indicating that the Y-Co catalyst is more active than

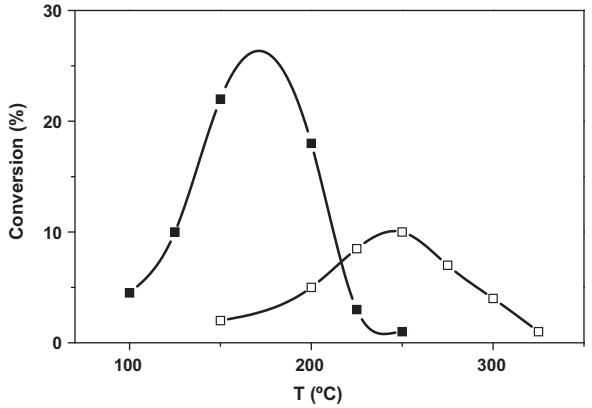

Fig. 2. Conversion-temperature curves for CCl_4 oxidation without water in the feed. (■) Y-Co, (□) Y-Cr. $W/F^0_{CCl_4} = 96$ g h mol^{-1}, $p_{CCl4} = 0.06$ atm, $p_{O2} = 0.10$ atm.

Y-Cr catalyst. The presence of the maximum in both cases is caused by the strong deactivation suffered by the catalysts.

After these catalytic tests all samples were characterized by XRD and nitrogen physisorption. As can be seen in Table 1, the values of *Sg* were one or two orders of magnitude lower than the fresh samples. In addition, the XRD patterns after reaction presented in Fig. 1B indicate that the cristallinity of the catalysts was very low compared to the fresh samples, showing even the presence of the amorphous halo corresponding to silica structure. These results are indicating that the oxidation of CCl_4 without water in the feed produces a total transformation in the structure of the exchanged Y-zeolite samples with an important loss of specific surface area and the crystalline structure of the zeolite. This phenomenon can be explained considering that during the oxidation of CCl_4 the only products that can be formed, when no water is present in the reactive mixture, are Cl_2 and CO_2. The gaseous Cl_2 formed probably was the responsible of the deactivation of the catalyst as a consequence of the dealuminization of the zeolite matrix [5,11].

3.3. Catalytic activity in presence of water in the feed

As it has been discussed above, the presence of water is critical to maintain the catalyst activity. Therefore, a set of experiments were carried out maintaining a partial pressure of water of 0.03 atm during the reaction. For each temperature analyzed, a fresh sample was used. In Fig. 3 are presented the results of the

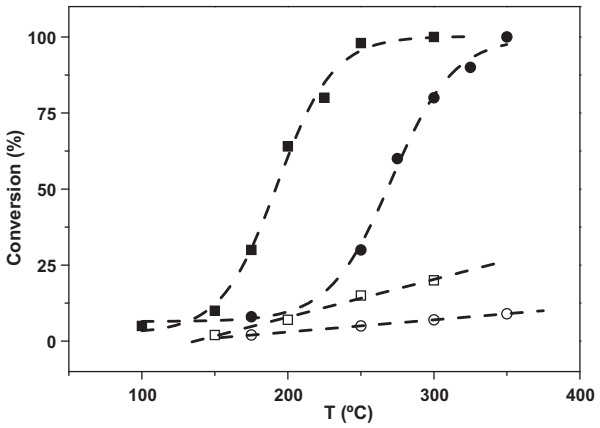

Fig. 3. Conversion-temperature curves for CCl_4 oxidation in the presence of water. (■) Y-Co, (●) Y-Cr, (□) Y-Fe, (○) Y-Mn. $W/F^0_{CCl_4} = 96$ g h mol^{-1} $p_{CCl4} = 0.06$ atm, $p_{O2} = 0.10$ atm, $p_{H2O} = 0.03$ atm.

evolution of CCl_4 conversion vs. reaction temperature. For the Y-Co sample the reaction started at 100 °C and the conversion increases with temperature, attaining 100% of conversion at 250 °C. For Y-Cr catalyst the CCl_4 combustion began at higher temperature, 175 °C, than Y-Co catalyst and 100% of CCl_4 conversion was reached at 350 °C. Furthermore, the values of the temperature needed to attain the 50% of conversion, T^{50}, were 190 and 270 °C for Y-Co and Y-Cr, respectively. Even considering that metal loading for Y-Co sample is higher than for Y-Cr sample, the reaction rate expressed by gram of metal remained higher for Y-Co than Y-Cr. All these results clearly indicate that Y-Co catalyst was more active than Y-Cr catalyst in CCl_4 oxidation. The other samples studied, Y-Mn and Y-Fe catalysts, had very low activity in the range of temperatures studied.

After catalytic tests the samples were also analyzed by nitrogen physisorption, atomic absorption (metal loading) and XRD. The values of the *Sg* shown in Table 1 indicate that are higher than those for the samples evaluated without water in the feed. In the same way, the XRD results see Fig. 1C, shows that the cristallinity of the samples was not affected. In summary, the presence of water in the reaction atmosphere is necessary to preserve the structure of the catalysts and consequently maintain their stability.

3.4. Kinetic study of carbon tetrachloride oxidation

Some previous experiments were carried out in transient conditions and it was found that Y-Co was the most active catalyst in the CCl_4 oxidation. Therefore, a kinetic study and modeling of CCl_4 combustion at different temperatures and low conversion conditions over Y-Co catalyst were carried out. The kinetic study was made under differential conditions; conversions were always lower 10%.

3.4.1. Influence of the oxygen partial pressure

The operating temperature was kept constant at 120 °C. The experiments were performed at CCl_4 partial pressure constant of 0.06 atm and water partial pressure constant of 0.03 atm and varying oxygen partial pressure between 0.05 and 0.18 atm. The presence of water in the feed is important in order to avoid the deactivation of the catalyst; probably restoring the Brönsted acid sites. Fig. 4 shows that the reaction rate of CCl_4 oxidation under these conditions remains constant.

3.4.2. Influence of the CCl_4 partial pressure

In order to determine the effect of the CCl_4 partial pressure, the oxygen partial pressure and water partial pressure were kept constant at 0.120 atm and 0.03 atm, respectively. The CCl_4 partial pressure was varied between 0.035 atm and 0.120 atm. These

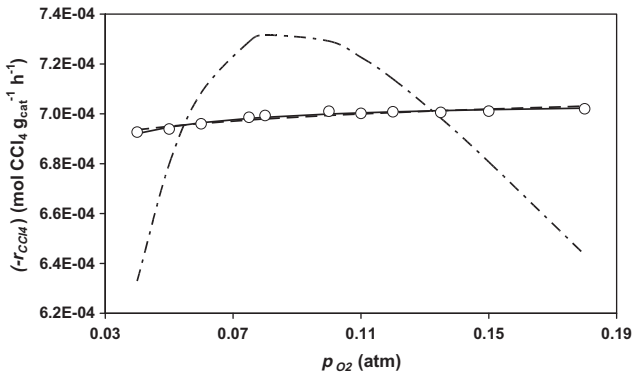

Fig. 4. Influence of O_2 concentration over the reaction rate. Y-Co catalyst. (○) experimental data, (-·-·-) SS-LHHW model predictions, (——) potential model predictions, (—) DS-LHHW model predictions.

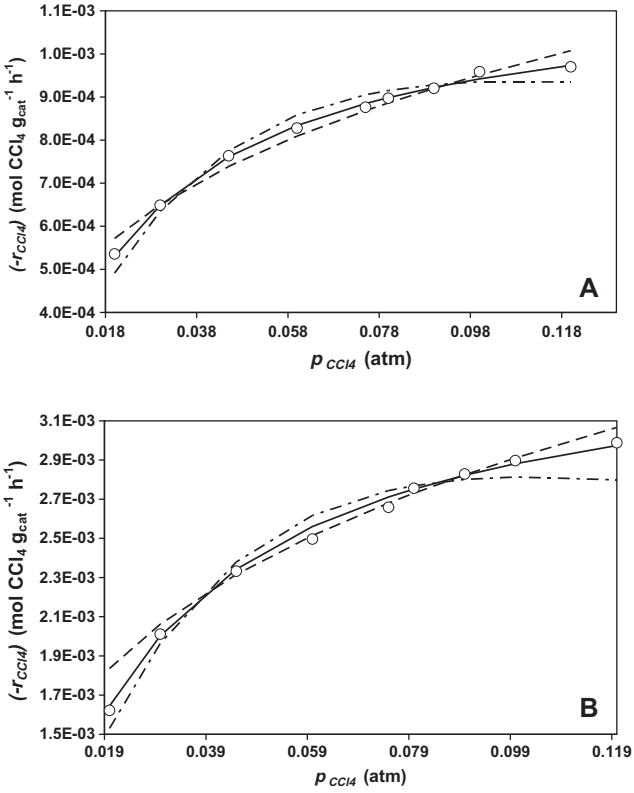

Fig. 5. Influence of CCl_4 concentration over the reaction rate. Y-Co catalyst. (A) corresponding to 120 °C, (B) corresponding to 130 °C. (○) experimental data, (-·-·-) SS-LHHW model predictions, (——) potential model predictions, (—) DS-LHHW model predictions.

experiments were carried out at two temperatures: 120 and 130 °C. Fig. 5 shows the results of the rate of reaction as a function of the CCl_4 partial pressure for Y-Co catalyst. It can be noticed that the rate of reaction increases with the CCl_4 partial pressure in a non-linear form, this behavior is indicative of a kinetic order between 0 and 1.

3.4.3. Influence of temperature

To analyze the effect of temperature on the rate of reaction, a series of experiments at different temperatures between 90 and 130 °C were performed. The reaction conditions were: constant oxygen partial pressure of 0.120 atm, constant CCl_4 partial pressure of 0.06 atm and constant water partial pressure of 0.03 atm. Reaction rate values were obtained from the conversion experiments as a function of time, taking the values of the initial conversion for each temperature under study.

3.5. Kinetic modeling of carbon tetrachloride oxidation

The experimental results of the kinetic study have been analyzed using empirical and mechanistic approaches. The kinetic models used are pseudo homogeneous power-law type and of LHHW type.

3.5.1. Pseudo homogeneous power-law type

According to the empirical power-law model, the reaction rate can be expressed as:

$$(-r_{CCl_4}) = k_P \cdot p_{O_2}^{\alpha} \cdot p_{CCl_4}^{\beta} \quad (1)$$

where $(-r_{CCl_4})$ is the rate of CCl_4 oxidation, k_P is the kinetic constant of reaction according to this potential model, and α and β are the

kinetic orders with respect to oxygen and CCl_4 respectively. The orders α and β may take virtually all the values, integer, fractional, positive, negative, or zero. Elementary reactions have integer orders. However, for the case of non-elementary reactions the kinetic orders will generally assume non-integral values that are only valid within a narrow range of operating conditions where the experiments has been carried out.

In order to have initial estimations of the kinetic parameters, Eq. (1) can be linearized as follows:

$$\log(-r_{CCl_4}) = \log(k_P) + \alpha \cdot \log(p_{O_2}) + \beta \cdot \log(p_{CCl_4}) \quad (2)$$

As can be seen in Fig. 6 the order with respect to a given reactant can be estimated from the slope of the line in a double-log plot of the reaction rate vs. the reactant concentration. The values obtained from the linear regression of the experimental data to Eq. (2), have been used as initial guesses for calculation by non-linear regression using Eq. (1). The objective function to minimized is the sum of squared residuals (*SSR*), defined as:

$$SSR = \sum((-r_{CCl_4})_{exp} - (-r_{CCl_4})_{cal})^2 \quad (3a)$$

In Table 2 are presented the values of the kinetic parameters for the potential model, and the main statistical parameters obtained by non-linear regression. These statistical parameters are the standard error of the reaction rate, *S.E.* $(-r_{CCl_4})$, and the correlation coefficient, R^2, defined as follows respectively:

$$S.E.(-r_{CCl_4}) = \sqrt{\frac{\sum((-r_{CCl_4})_{exp} - (-r_{CCl_4})_{cal})^2}{(n-p)}}$$
$$R^2 = 1 - \frac{\sum((-r_{CCl_4})_{exp} - (-r_{CCl_4})_{cal})^2}{\sum((-r_{CCl_4})_{exp} - \overline{(-r_{CCl_4})_{exp}})^2} \quad (3b)$$

In the above expressions, n and p represent the number of experimental data, and the number of parameters of the model, respectively.

As can be observed in Figs. 4 and 5, the potential model, fits satisfactorily the experimental data and all the kinetic parameters are calculated with enough statistical precision. The values in Table 2 show that the kinetic orders, α and β are quite low, especially in the case of the order with respect oxygen (α). This value, which do not have a direct mechanistic meaning, is consequence of the very low influence of the oxygen concentration at the conditions studied [12]. This fact can be explained assuming a strong adsorption of O_2 molecule, leading to a high coverage of the catalyst surface [13]. In the case of the CCl_4, the value of β is also low, indicating again a clear effect of the adsorption of this compound over the catalyst surface. More interesting is the fact that the value of β changes with the reaction temperature.

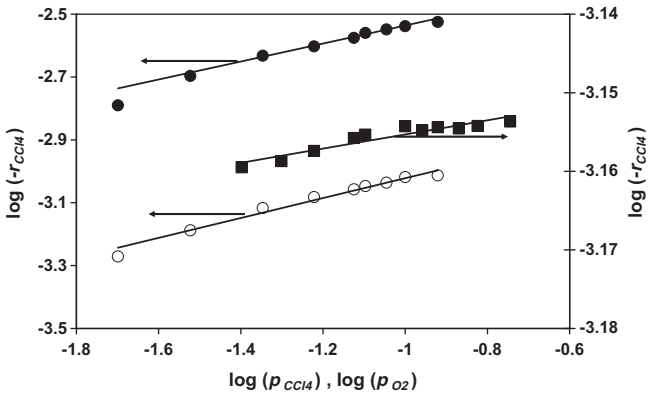

Fig. 6. Double-log plot of potential model. (●) effect of CCl_4 at 120 °C; (○) effect of CCl_4 at 130 °C; (■) effect of O_2 at 120 °C; Solid lines: linearized model.

Although the confidence intervals calculated for this parameter, see Table 2, show that this change could do not have a statistical significance, this change can be easily explained considering the decrease of the degree of CCl_4 adsorption as the reaction temperature increases [13]. The above facts indicate that there is a relationship between the values of the kinetic orders and the adsorption parameters that usually have been explained in a qualitative manner [13].

Fig. 7A shows the influence of reaction temperature on the reaction rate, in the interval from 90 to 130 °C, at constant the O_2 and CCl_4 concentrations. The modified Arrhenius plot, Fig. 7B, shows the good linearity in this interval of temperatures. The calculation of the apparent activation energy (E_a) has been also done by non-linear regression, using the re-parameterized form of the kinetic constant k_p:

$$k_P = k_{P_0} \cdot \exp\left(-\frac{E_a}{RT}\right) = k_{P_m} \cdot \exp\left(-E_a \cdot \left(\frac{T_m - T}{R \cdot T_m \cdot T}\right)\right)$$
$$k_{P_m} = k_{P_0} \cdot \exp\left(-\frac{E_a}{RT_m}\right); \quad T_m = 383 \text{ K} \quad (4)$$

The apparent activation energy obtained for the Y-Co catalyst was 98.2 ± 5.1 kJ mol^{-1}. From E_a and T_m values, the pre-exponential factor determined is $k_{P_0} = 9.24 \cdot 10^9$ h^{-1}. The estimated value of the activation energy is in the same order reported in the literature for catalytic combustion of CCl_4 over metal oxide catalysts on monolith support [4], and is the result of combined effect of the intrinsic activation energy, and the adsorption heats of O_2 and CCl_4 [14].

3.5.2. Langmuir Hinshelwood Hougen Watson (LHHW) model

On the other hand, the consideration of reactant adsorption steps to explain the mechanism of CCl_4 oxidation leads to the development of LHHW kinetic model. With this type of model we have considered two alternative cases:

1. Single-site case (SS-LHHW): The adsorption of CCl_4 and O_2 is competitive over only one type of active sites, denoted by $*$ and;
2. Double-site case (DS-LHHW): The adsorption of CCl_4 and O_2 is non-competitive, assuming the adsorption of each molecule over two different types of sites, denoted by *S* and *L* respectively. A bifunctional mechanism, including two types of sites, was proposed by Ramachandran et al. for the combustion of methylene chloride and carbon tetrachloride using metal-loaded zeolite catalysts [2].

In both cases it is also assumed that the oxygen adsorption is non-dissociative, and the surface reaction of CCl_4 oxidation is irreversible, attaining total combustion.

For the *SS-LHHW*, the main steps of the reaction mechanism are the following:

$$(i) \quad O_2 + * \overset{K_{O_2}}{\longleftrightarrow} O_2 - *; \quad K_{O_2} = \frac{[O_2 - *]}{p_{O_2} \cdot [*]} \quad (5)$$

$$(ii) \quad H_2O + * \overset{K_{H_2O}}{\longleftrightarrow} H_2O - *; \quad K_{H_2O} = \frac{[H_2O - *]}{p_{H_2O} \cdot [*]} \quad (6)$$

$$(iii) \quad CCl_4 + * \overset{K_{CCl_4}}{\longleftrightarrow} CCl_4 - *; \quad K_{CCl_4} = \frac{[CCl_4 - *]}{p_{CCl_4} \cdot [*]} \quad (7)$$

$$(iv) \quad CCl_4 - * + O_2 - * \overset{k}{\underset{SS}{\longrightarrow}} CO_2(g) + 2Cl_2(g) + 2*; \quad (-r_{CCl_4})$$

Supposing that the rate determining step is the surface chemical reaction, step (*iv*), the reaction rate can be calculated as:

$$(-r_{CCl_4}) = k_{SS} \cdot [CCl_4 - *] \cdot [O_2 - *] \quad (8)$$

Table 2
Kinetic parameters for Co catalyst. Potential Model.

Parameter	Value	Standard error	Confidence interval (95%)	Lower limit	Upper limit
O_2 influence					
k_p (120 °C)	7.140E−04	1.780E−06	4.027E−06	7.100E−04	7.180E−04
α (120 °C)	0.0090	0.0010	0.0023	0.0067	0.0113
R^2 = 0.896			S.E. $(-r_{CCl_4})$ = 1.072E−06		
CCl_4 influence					
k_p (120 °C)	1.970E−03	1.049E−04	2.479E−04	1.722E−03	2.218E−03
β (120 °C)	0.316	0.020	0.047	0.269	0.363
R^2 = 0.977			S.E. $(-r_{CCl_4})$ = 2.357E−05		
k_p (130 °C)	5.627E−03	3.633E−04	8.591E−04	4.768E−03	6.486E−03
β (130 °C)	0.286	0.024	0.057	0.230	0.343
R^2 = 0.960			S.E. $(-r_{CCl_4})$ = 2.363E−05		
Temperature influence					
k_m (Tm)	3.705E−04	2.512E−05	5.941E−05	3.111E−04	4.299E−04
E_a (kJ/mol)	98.2	5.1	12.2	86.1	110.4
	R^2 = 0.991		S.E. $(-r_{CCl_4})$ = 5.739E−05		
Tm=110 °C					

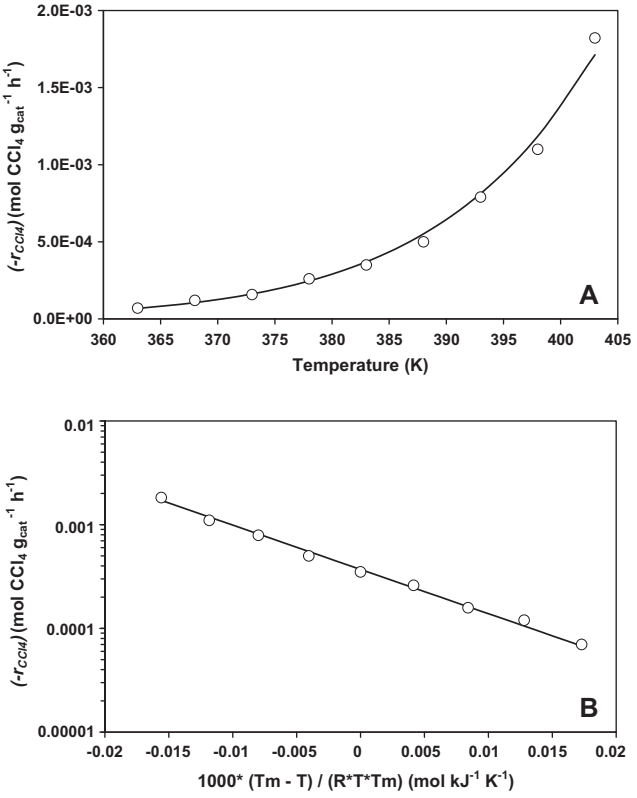

Fig. 7. Influence of reaction temperature over the reaction rate (A). Modified Arrhenius plot (B). (○) experimental data, (—) calculated data.

The term k_{SS} represents the intrinsic kinetic constant for the single-site case. Now, the balance of the active sites is given by:

$$[*_T] = [*] + [O_2 - *] + [CCl_4 - *] + [H_2O - *] \quad (9)$$

Substituting Eqs. (5), (6), (7), and (9) into Eq. (8), the reaction rate can be expressed as follows:

$$(-r_{CCl_4}) = \frac{k_{SS} \cdot K_{CCl_4} \cdot K_{O_2} \cdot [*_T]^2 \cdot p_{CCl_4} \cdot p_{O_2}}{(1 + K_{O_2} \cdot p_{O_2} + K_{H_2O} \cdot p_{H_2O} + K_{CCl_4} \cdot p_{CCl_4})^2} \quad (10)$$

For the case of experiments carried out at constant oxygen concentration, and remembering that the water concentration also was maintained constant during the reaction, Eq. (10) can be simplified to:

$$(-r_{CCl_4}) = \frac{k'_{SS} \cdot p_{CCl_4}}{(1 + K'_{CCl_4} \cdot p_{CCl_4})^2} \quad (11)$$

where the lumped parameters k'_{SS} and K'_{CCl_4} are defined by:

$$k'_{SS} = \frac{k_{SS} \cdot K_{CCl_4} \cdot K_{O_2} \cdot [*_T]^2 \cdot p_{O_2}}{(1 + K_{O_2} \cdot p_{O_2} + K_{H_2O} \cdot p_{H_2O})^2}$$
$$K'_{CCl_4} = \frac{K_{CCl_4}}{(1 + K_{O_2} \cdot p_{O_2} + K_{H_2O} \cdot p_{H_2O})^2} \quad (12)$$

Eq. (11) can be linearized as follows, Fig. 8, to obtain initial guess of the lumped kinetic parameters k'_{SS} and K'_{CCl_4}, gives:

$$\sqrt{\frac{p_{CCl_4}}{(-r_{CCl_4})}} = \frac{1}{\sqrt{k'_{SS}}} + \frac{K'_{CCl_4}}{\sqrt{k'_{SS}}} \cdot p_{CCl_4} \quad (13)$$

On the other hand, in the case of the experiments carried out at constant CCl_4 concentration, Eq. (10) is simplified to:

$$(-r_{CCl_4}) = \frac{k''_{SS} \cdot p_{O_2}}{(1 + K''_{O_2} \cdot p_{O_2})^2} \quad (14)$$

Now, the terms k''_{SS} and K''_{O_2} are given by:

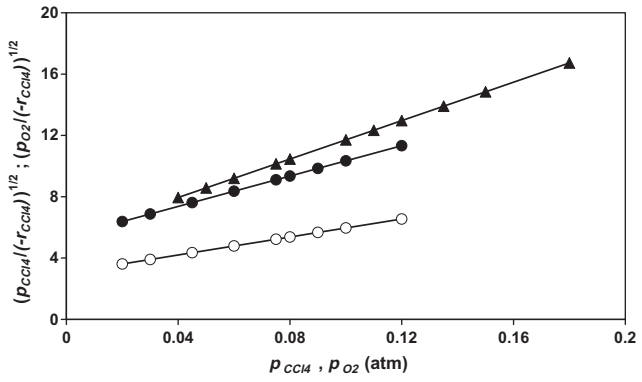

Fig. 8. Linearized plot of LHHW-SS model. (●): effect of CCl_4 at 120 °C; (○): effect of CCl_4 at 130 °C, (▲) effect of O_2 at 120 °C; Solid lines: linearized model.

$$k''_{SS} = \frac{k_{SS}\cdot K_{CCl_4}\cdot K_{O_2}\cdot[*T]^2\cdot p_{CCl_4}}{(1+K_{H_2O}\cdot p_{H_2O}+K_{CCl_4}\cdot p_{CCl_4})^2}$$
$$K''_{O_2} = \frac{K_{O_2}}{(1+K_{CCl_4}\cdot p_{CCl_4}+K_{H_2O}\cdot p_{H_2O})^2} \quad (15)$$

In the same way, the estimation of the initial kinetic parameters, k''_{SS} and K''_{O_2}, are obtained as follows (see Fig. 8):

$$\sqrt{\frac{p_{O_2}}{(-r_{CCl_4})}} = \frac{1}{\sqrt{k''_{SS}}} + \frac{K''_{O_2}}{\sqrt{k''_{SS}}}\cdot p_{O_2} \quad (16)$$

Table 3 reports the kinetic and the statistical parameters corresponding to SS-LHHW model. It can be seen that the values of K''_{O_2} increase with temperature which has not physical meaning. The fitting of the experimental data with SS-LHHW (Figs. 4 and 5) was not satisfactory.

In the DS-LHHW model, is considered that the active sites, named *S*, are responsible for oxygen and water adsorption, and that the adsorption of CCl_4 occurs over active sites denoted as *L*. The sequence of steps assumed for this mechanism are the following:

$$(i)\quad O_2(g) + S \overset{K_{O_2}}{\longleftrightarrow} O_2 - S; \quad K^S_{O_2} = \frac{[O_2 - S]}{p_{O_2}\cdot[S]} \quad (17)$$

$$(ii)\quad H_2O + S \overset{K_{H_2O}}{\longleftrightarrow} H_2O - S; \quad K^S_{H_2O} = \frac{[H_2O - S]}{p_{H_2O}\cdot[S]} \quad (18)$$

$$(iii)\quad CCl_4 + L \overset{K_{CCl_4}}{\longleftrightarrow} CCl_4 - L; \quad K^L_{CCl_4} = \frac{[CCl_4 - L]}{p_{CCl_4}\cdot[L]} \quad (19)$$

$$(iv)\quad CCl_4 - L + O_2 - S \overset{k_{DS}}{\rightarrow} CO_2(g) + 2Cl_2(g) + S + L; \quad (-r_{CCl_4})$$

Assuming that the rate determining step is the surface chemical reaction, the reaction rate is given by the following expression:

$$(-r_{CCl_4}) = k_{DS}\cdot[CCl_4 - L]\cdot[O_2 - S] \quad (20)$$

The term k_{DS} represents the intrinsic kinetic constant according to the *DS-LHHW* mechanism. The balances of active sites *S* and *L* are given respectively by:

$$[S_T] = [S] + [O_2 - S] + [H_2O - S] = [S]\cdot(1 + K^S_{O_2}\cdot p_{O_2} + K^S_{H_2O}\cdot p_{H_2O}) \quad (21)$$

$$[L_T] = [L] + [CCl_4 - L] = [L]\cdot(1 + K^L_{CCl_4}\cdot p_{CCl_4}) \quad (22)$$

where S_T and L_T represent the concentration of total sites for O_2 and H_2O, and for CCl_4, respectively.

Finally, substituting Eqs. (17), (18), (19), (21) and (22) in Eq. (20), the reaction rate results:

$$(-r_{CCl_4}) = \frac{k_{DS}\cdot K_{O_2}\cdot K_{H_2O}\cdot[L_T]\cdot[S_T]\cdot p_{O_2}\cdot p_{CCl_4}}{(1 + K^L_{CCl_4}\cdot p_{CCl_4})\cdot(1 + K^S_{O_2}\cdot p_{O_2} + K^S_{H_2O}\cdot p_{H_2O})} \quad (23)$$

When the partial pressures of oxygen and water are maintained constant during the reaction, the above expression can be simplified as follows:

$$(-r_{CCl_4}) = \frac{k'_{DS}\cdot p_{CCl_4}}{(1 + K^L_{CCl_4}\cdot p_{CCl_4})} \quad (24)$$

where the term k'_{DS} is:

$$k'_{DS} = \frac{k_{DS}\cdot K^S_{O_2}\cdot K^S_{H_2O}\cdot[L_T]\cdot[S_T]\cdot p_{O_2}}{(1 + K^S_{O_2}\cdot p_{O_2} + K^S_{H_2O}\cdot p_{H_2O})} \quad (25)$$

Now, the initial estimation of the parameters k'_{DS} and $K^L_{CCl_4}$ can be done by linearization of Eq. (24), see Fig. 9:

$$\frac{p_{CCl_4}}{(-r_{CCl_4})} = \frac{1}{k'_{DS}} + \frac{K^L_{CCl_4}}{k'_{DS}}\cdot p_{CCl_4} \quad (26)$$

When the experiments were carried out at constant partial pressure of CCl_4, Eq. (23) becomes:

$$(-r_{CCl_4}) = \frac{k''_{DS}\cdot p_{O_2}}{(1 + K^{S\prime\prime}_{O_2}\cdot p_{O_2})} \quad (27)$$

where the terms k''_{DS} and $K^{S\prime\prime}_{O_2}$ are defined by:

$$k''_{DS} = \frac{k_{DS}\cdot K^L_{CCl_4}\cdot K^S_{O_2}\cdot[L_T]\cdot[S_T]\cdot p_{CCl_4}}{(1+K^L_{CCl_4}\cdot p_{CCl_4})\cdot(1+K^S_{H_2O}\cdot p_{H_2O})}$$
$$K^{S\prime\prime}_{O_2} = \frac{K^S_{O_2}}{(1+K^S_{H_2O}\cdot p_{H_2O})} \quad (28)$$

k''_{DS} and $K^{S\prime\prime}_{O_2}$ can be evaluated using the following linear expression, see Fig. 9:

$$\frac{p_{O_2}}{(-r_{CCl_4})} = \frac{1}{k''_{DS}} + \frac{K^{S\prime\prime}_{O_2}}{k''_{DS}}\cdot p_{O_2} \quad (29)$$

Table 4 shows the kinetic and the statistical parameters corresponding to model DS-LHHW. The fittings obtained with this model are shown in Figs. 4 and 5.

Since the number of parameters is the same in all models, a direct comparison of *S.E.* $(-r_{CCl_4})$ values (Eq. (3a)) can be used to discriminate among them and select the best model. From the *S.E.* values in Tables 2–4 it can be seen that the best fitting was obtained with the DS-LHHW model. According to this mechanism, two active sites are involved on the controlling step of the reaction mechanism. These active sites correspond to the adsorption of O_2 and water, and to the adsorption of CCl_4 respectively. Chatterjee et al. [16] suggest that the oxidation of CCl_4 involves an intermediate step producing posghene and Cl_2, and this posghene, on a further reaction with adsorbed oxygen or water, produces CO_2. Furthermore, Ramachandran et al. [2], have shown that phosgene is a reaction intermediate in the catalytic abatement of CCl_4 on

Table 3
Kinetic parameters for Co catalyst. Single Site LHHW Model.

Parameter	Value	Standard error	Confidence interval (95%)	Lower limit	Upper limit
O_2 influence					
k''_{SS} (120 °C)	0.0338	0.0026	0.0058	0.0279	0.0396
K''_{O_2} (120 °C)	11.518	0.838	1.897	9.622	13.415
R^2 = 0.512			S.E. $(-r_{CCl_4})$ = 3.527E−05		
CCl_4 influence					
k'_{SS} (120 °C)	0.0344	0.0018	0.0042	0.0302	0.0386
K'_{CCl4} (120 °C)	9.183	0.569	1.345	7.839	10.528
R^2 = 0.964			S.E. $(-r_{CCl_4})$ = 2.990E−05		
k'_{SS} (130 °C)	0.1090	0.0065	0.0154	0.0936	0.1245
K'_{CCl4} (130 °C)	9.686	0.683	1.615	8.072	11.301
R^2 = 0.997			S.E. $(-r_{CCl_4})$ = 2.477E−05		

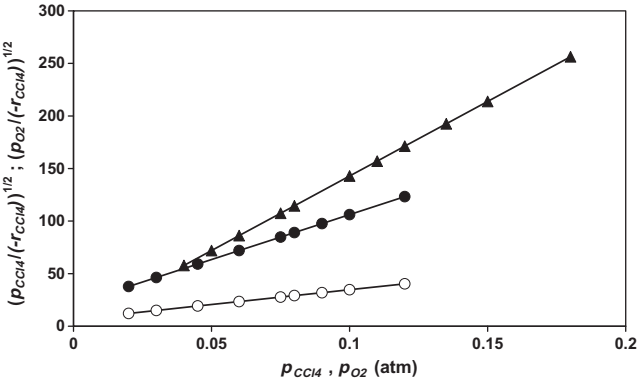

Fig. 9. Linearized plot of LHHW-DS model. (●): effect of CCl_4 at 120 °C; (○): effect of CCl_4 at 130 °C, (▲) effect of O_2 at 120 °C; Solid lines: linearized model.

Table 4
Kinetic parameters for Co catalyst. Dual Site LHHW Model.

Parameter	Value	Standard error	Confidence interval (95%)	Lower limit	Upper limit
O_2 influence					
k'_{DS} (120 °C)	0.926	0.061	0.138	0.787	1.064
$K^{S''}_{O_2}$ (120 °C)	1312.44	87.55	198.06	1114.38	1510.50
R^2 = 0.960			S.E. $(-r_{CCl_4})$ = 6.68E−07		
CCl_4 influence					
k'_{DS} (120 °C)	0.049	0.001	0.003	0.046	0.051
K^{L}_{CCl4} (120 °C)	43.53	1.37	3.24	38.28	44.77
R^2 = 0.997			S.E. $(-r_{CCl_4})$ = 7.917E−06		
k'_{DS} (130 °C)	0.153	0.005	0.013	0.141	0.166
K^{L}_{CCl4} (130 °C)	41.22	2.01	4.74	38.48	47.97
R^2 = 0.998			S.E. $(-r_{CCl_4})$ = 7.662E−06		

exchanged Co-zeolite; and Sinquin et al. [17] have reported that the formed phosgene can then readily react with water, or with surface OH^- groups to produce HCl and CO_2. These authors also proposed that water could regenerate the catalytic active sites which were poisoned by Cl_2, in accordance with our results.

3.6. Analytic relationships between the kinetic models

According to the methodology proposed by Monzón et al. [15], it can be deduced analytical expressions between the parameters of the different kinetic models. These analytical expressions can be also used to check the validity of the obtained parameters, and to select the most appropriated model. As is pointed out by Chorkendorff and Niemantsverdiert [14], the kinetic order of a potential model can be estimated from the logarithmic derivative of the reaction rate with respect to the variable considered. For example, in the Potential model, Eq. (1), the effect of O_2 and CCl_4 concentrations are given by the values of α and β respectively. As is presented in Fig. 6, these values can be calculated from the following logarithmic derivatives:

$$\beta = \frac{d(\log(-r_{CCl_4}))}{d(\log(p_{CCl_4}))} = \left(\frac{d(-r_{CCl_4})}{dp_{CCl_4}}\right) \cdot \frac{p_{CCl_4}}{(-r_{CCl_4})}; p_{O_2} = const. \quad (30)$$

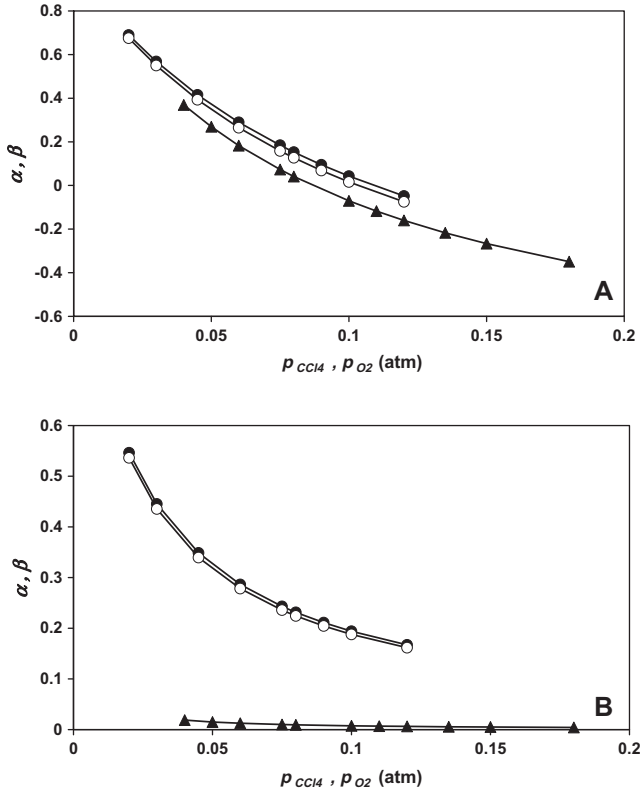

Fig. 10. Effect of CCl_4 and O_2 concentration over the calculated kinetic orders. LHHW-SS model (A); LHH-DS model (B). (●): effect of CCl_4 at 120 °C; (○): effect of CCl_4 at 130 °C, (▲) effect of O_2 at 120 °C.

$$\alpha = \frac{d(\log(-r_{CCl_4}))}{d(\log(p_{O_2}))} = \left(\frac{d(-r_{CCl_4})}{dp_{O_2}}\right) \cdot \frac{p_{O_2}}{(-r_{CCl_4})}; \quad p_{CCl_4} = const. \quad (31)$$

By calculation of the corresponding derivatives of $(-r_{CCl_4})$, Eq. (10), the following analytical expression between α and β, and the adsorption parameters of the SS-LHHW model is deduced:

$$\alpha = \left(\frac{1 - K''_{O_2} \cdot p_{O_2}}{1 + K''_{O_2} \cdot p_{O_2}}\right); \quad \beta = \left(\frac{1 - K'_{CCl_4} \cdot p_{CCl_4}}{1 + K'_{CCl_4} \cdot p_{CCl_4}}\right) \quad (32)$$

Similarly, for the *DS-LHHW* model the expressions for α and β are:

$$\alpha = \left(\frac{1}{1 + K^{S''}_{O_2} \cdot p_{O_2}}\right); \quad \beta = \left(\frac{1}{1 + K^{L}_{CCl_4} \cdot p_{CCl_4}}\right) \quad (33)$$

Using the corresponding values of adsorption constants shown in Tables 3 and 4, (Eqs. (32) and (33)) the variation of the kinetic orders, α and β, with respect to the O_2 and CCl_4 concentrations, can be calculated for both models respectively (see Fig. 10).

The results obtained with the SS-LHHW model, Eq. (32), indicate that α can take values from −1, when $K''_{O_2} \cdot p_{O_2} \gg 1$, to 1, when $K''_{O_2} \cdot p_{O_2} \ll 1$. A similar analysis can be done for β. In the interval from −1 to 1, are included the values of α and β in Table 2. However, if we calculate the average values of the orders predicted by Eq. (32), the results are the following: α (at 120 °C) = −0.077; β (at 120 °C) = 0.251 and β (at 130 °C) = 0.226. The main difference is observed in the value of α, because Eq. (32) predicts that at high O_2 concentrations this order takes negative values, see Fig. 10. At high CCl_4 concentrations, slightly negative values of β can be obtained.

However, for the case of the DS-LHHW model, α and β can vary from 0 to 1. Again, this interval includes the values of α and β

presented in Table 2. But, in this case, the average values predicted by Eq. (33) are: α (at 120 °C) = 0.081, β (at 120 °C) 0.285 and β (at 130 °C)=0.277. These are quite close to that obtained with the Potential model, confirming the goodness of the DS-LHHW model.

In summary, from Eqs. (32) and (33) it can be seen that the kinetic orders, determined by power-law model type, strongly depend on the operating conditions: reaction temperature and the feed composition. In consequence in an integral reactor, which operate at high reactant conversions, the observable kinetic orders vary from the entrance to the exit because the composition of the reactant phase is changing along the reactor, even under operation at isothermal conditions. Therefore, the applicability of these models is usually restricted to narrow intervals of operation.

4. Conclusions

From the results presented in this contribution it can be concluded that Y-Co and Y-Cr catalysts are active for CCl_4 oxidation at atmospheric pressure and low temperatures. The most active of the tested catalyst was the Y-Co sample. Thus, at 150 °C the conversion of CCl_4 attained with this catalyst was one order of magnitude higher than the conversion attained with Y-Cr catalyst. The presence of water in the reaction atmosphere is necessary to avoid the destruction of the zeolite matrix and maintain the catalyst activity. The kinetic modeling developed indicates that the low influence of the CCl_4 partial pressure, and especially of the oxygen concentration, can be explained assuming strong adsorption effect over the surface of the catalyst. All the kinetics results obtained can be satisfactorily explained assuming a mechanism, denoted as DS-LHHW, involving the adsorption of O_2 and CCl_4 on two different types of sites. The direct relationships between the kinetic parameters of the different models has been deduced. These relationships clearly explain the variations observed of the kinetic orders with the operating conditions.

Acknowledgments

We thank the Universidad Nacional del Litoral (UNL), Consejo Nacional de Investigaciones Científicas y Técnicas (CONICET) and Agencia Nacional de Promoción Científica y Tecnológica (ANPCyT), Argentina for the financial support of this work.

References

[1] G. Erlt, H. Knözinger, F. Schüth, J. Weitkamp (Eds.), Handbook of Heterogeneous Catalysis, second ed., Wiley-VCH, Weinheim, 2008.
[2] B. Ramachandran, H.L. Greene, S. Chatterjee, Decomposition characteristics and reaction mechanisms of methylene chloride and carbon tetrachloride using metal-loaded zeolite catalysts, Appl. Catal. B: Environ. 8 (1996) 157–182.
[3] S. Imamura, H. Tarumoto, S. Ishida, Decomposition of 1,2-dichloroethane on titanium dioxide/silica, Ind. Eng. Chem. Res. 28 (1989) 1449–1455.
[4] T. Tanilmis, S. Atalay, H. Arden Alpay, F. Sami Atalay, Catalytic combustion of carbon tetrachloride, J. Hazard. Mater. B90 (2002) 157–167.
[5] A. Aranzabal, J.L. Ayastuy-Arizti, J.A. González-Marcos, J.R. González-Velasco, The reaction pathway and kinetic mechanism of the catalytic oxidation of gaseous lean TCE on Pd/alumina catalysts, J. Catal. 214 (2003) 130–135.
[6] B. Miranda, E. Díaz, S. Ordoñez, F.V. Díez, Catalytic combustion of trichloroethene over Ru/Al2O3: reaction mechanism and kinetic study, Catal. Commun. 7 (2006) 945–949.
[7] R. López-Fonseca, B. de Rivas, J.I. Gutiérrez-Ortiz, A. Aranzabal, J.R. González-Velasco, Enhanced activity of zeolites by chemical dealumination for chlorinated VOC abatement, Appl. Catal. B: Environ. 41 (2003) 31–42.
[8] B. Rivas, R. López-Fonseca, C. Jiménez-González, J.I. Gutiérrez-Ortiz, Highly active behaviour of nanocrystalline Co_3O_4 from oxalate nanorods in the oxidation of chlorinated short chain alkanes, Chem. Eng. J. 184 (2012) 184–192.
[9] S. Gil, M. Marchena, L. Sánchez-Silva, A. Romero, P. Sánchez, J.L. Valverde, Effect of the operation conditions on the selective oxidation of glycerol with catalysts based on Au supported on carbonaceous materials, Chem. Eng. J. 178 (2011) 423–435.
[10] C.I. Meyer, A. Borgna, A. Monzón, T.F. Garetto, Kinetic study of trichloroethylene combustion on exchanged zeolites catalysts, J. Hazard. Mater. 190 (2011) 903–908.
[11] A. Gervasini, C. Pirola, S. Zilio, V. Ragaini, Destruction of carbon tetrachloride in the presence of hydrogen-supplying compounds with ionisation and catalytic oxidation: Part 2. Methane as hydrogen font, Appl. Catal. B: Environ. 47 (2004) 257–267.
[12] M. Boudart, G. Djéga-Mariadassou, Kinetics of Heterogenous Catalytic Reactions, Princeton University Press, Princeton, NJ, USA, 1984.
[13] K. Tamaru, M. Boudart, H.S. Taylor, The thermal decomposition of germane. I. Kinetics, J. Phys. Chem. 59 (1955) 801–805.
[14] I. Chorkendorff, J.W. Niemantsverdiert, Concepts of Modern Catalysis and Kinetics, Willey-VCH, Weinheim (Germany), 2003.
[15] A. Monzón, E. Romeo, A. Borgna, Relationship between the kinetic parameters of different catalyst deactivation models, Chem. Eng. J. 94 (2003) 19–28.
[16] S. Chatterjee, H.L. Greene, Y. Joon Park, Comparison of modified transition metal-exchanged zeolite catalysts for oxidation of chlorinated hydrocarbons, J. Catal. 138 (1992) 179–194.
[17] G. Sinquin, C. Petit, S. Libs, J.P. Hindermann, A. Kiennemann, Catalytic destruction of chlorinated C1 volatile organic compounds (CVOCs) reactivity, oxidation and hydrolysis mechanisms, Appl. Catal. B: Environ. 27 (2000) 105–115.